



LAFAYETTE

SENIOR HONORS THESIS

DEPARTMENT OF MECHANICAL ENGINEERING

Interaction of Cavity Frequencies in Supersonic Combustible Flow

Author:

D. Mac JONES

Advisor:

Dr. Tobias ROSSMANN

Thesis Committee:

Dr. Tobias Rossmann, Chair

Mechanical Engineering

Dr. Daniel Sabatino

Mechanical Engineering

Dr. James Schaefer

Chemical and Biomolecular Engineering

*A thesis submitted in fulfillment of the requirements
for Honors in Mechanical Engineering
in the*



April 2016

Declaration of Authorship

I, D. Mac JONES, declare that this thesis titled, 'Interaction of Cavity Frequencies in Supersonic Combustible Flow' and the work presented in it are my own. I confirm that:

- This work was done wholly or mainly while in candidature for a research degree at this University.
- Where any part of this thesis has previously been submitted for a degree or any other qualification at this College or any other institution, this has been clearly stated.
- Where I have consulted the published work of others, this is always clearly attributed.
- Where I have quoted from the work of others, the source is always given. With the exception of such quotations, this thesis is entirely my own work.
- I have acknowledged all main sources of help.
- Where the thesis is based on work done by myself jointly with others, I have made clear exactly what was done by others and what I have contributed myself.

Signed:

Date:

“60% of the time, it works every time.”

Brian Fantana

Abstract

**Interaction of Cavity Frequencies in Supersonic
Combustible Flow**

by D. Mac JONES

LAFAYETTE COLLEGE

Honors in Mechanical Engineering

The Thesis Abstract is written here (and usually kept to just this page or so . . .)

Acknowledgements

The acknowledgements and the people to thank go here, don't forget to include your project advisor...

Contents

Declaration of Authorship	i
Abstract	iii
Acknowledgements	iv
Contents	v
List of Figures	vii
List of Tables	viii
Abbreviations	ix
Physical Constants	x
Symbols	xi
1 Introduction	1
1.1 Motivation	1
1.1.1 Subsection 1	3
1.1.2 Subsection 2	4
1.2 Main Section 2	4
2 Experimental Setup	6
2.1 Expansion Tube	6
2.1.1 Sections	6
2.1.2 Diaphragms	7
2.1.3 •	10
2.2 Models	10
2.2.1 Overview and Design Choices	10
2.2.2 Modular Design	10
2.2.3 Implementation	11
2.3 High Speed Pressure Transducers	11
2.3.1 Circuit	12
2.3.2 Implementation and Troubleshooting	12
2.4 Infrared Sensor	12
2.4.1 Alignment	12

2.4.2 Calibration	12
2.4.3 Operation	12
2.5 Schlieren Imaging	13
 A Appendix Title Here	 19
 Bibliography	 20

List of Figures

1.1	Diagram of typical cavity	5
2.1	Annotated Expansion Tube	15
2.2	Cavity 3D Model	16
2.3	Cavity Model with Inserts	16
2.4	IR setup diagram	17
2.5	Labeled photograph of IR setup	17
2.6	Schlieren Diagram	18

List of Tables

2.1 Diaphragm Burst Pressures	8
---	---

Abbreviations

L/D Length to Depth ratio

fps Frames Per Second

TTL Transistor Transistor Logic

Physical Constants

Speed of Light c = $2.997\ 924\ 58 \times 10^8$ ms⁻¹ (exact)

Symbols

a	distance	m
P	power	W (Js ⁻¹)
ω	angular frequency	rads ⁻¹

For/Dedicated to/To my...

Chapter 1

Introduction

1.1 Motivation

Scramjet engines are on the forefront of supersonic transportation development because of their simplicity and promising outlook for steady and reliable supersonic combustion. These engines differ from typical subsonic jet engines, as scramjets have no moving parts and simply rely on shock waves produced at these supersonic speeds to compress the intake air and provide the means for ignition.

One challenge facing the production of these engines is producing steady combustion. Much like keeping a match lit in a hurricane, keeping a flame stabilized at supersonic speeds is difficult. One proposed method of flame stabilization is a rectangular cavity. These cavities, like the cavity shown in Figure ??, are able to provide a re-circulation zone with high temperatures and combustion radicals for strong combustion to occur. Many experimental studies have tested the flame-holding abilities of cavities in strong combustion cases [1–4]. Strong combustion occurs when the fuel-air mixture is optimized for efficient fuel burning. The mixture in strong combustion cases occurs in proper

stoichiometric proportions. These studies focused on cavity dimensions and how the length to depth ratio, L/D, affects key ignition and flame holding characteristics, such as stagnation pressure, stagnation temperature, fuel air mixture, and residence time. Ben-Yakar concluded that with L/D ratios between 4 and 10, strong combustion can be sustained in these cavities for total enthalpy flight conditions of Mach 8, 10, and 13[2]. Also noted in several investigations is the presence of strong acoustic waves[5–10].

Similar to blowing air over an empty bottle to create a tone, the freestream air traveling over and interacting with these cavities produces acoustic waves. In these cavities, a shear layer develops between the high speed freestream and the slower, re-circulating air in the cavity. As the shear layer travels downstream, it begins to drop. By the time the shear layer reaches the downstream wall of the cavity, it has lowered to a point where the interaction of the shear layer with the downstream wall of the cavity produces strong pressure waves, which propagate upstream, ultimately resonating within the cavity.

Other experimental studies have investigated the acoustic properties of these cavities [5–10]. These investigations concluded that the acoustic waves generated by supersonic cavities produce several undesirable effects. One effect, investigated by McGregor is the induced drag associated with rectangular cavities. The effect of pressure waves within these cavities can increase the drag by as much as 250% [8]. These acoustic waves can also have an adverse effect on equipment and the crew. At low frequencies, the resonating acoustic waves can cause structural damage to the engine. At high frequencies, these waves can cause uneasiness in crew members [8].

Conclusions drawn from these investigations have led to the desire to suppress these acoustic waves. Suppressing these waves would reduce drag on the engine and cause less damage to the engine or the crew. However, these acoustic waves could have the

potential to assist in combustion when conditions for weak combustion are present. Weak combustion, as is studied in this investigation, is at lean fuel air mixture conditions. Sato et al.[10] investigated the enhancement of mixing due to acoustic waves. They concluded that mixing was enhanced by these acoustic waves and the rate of enhancement was controlled by the cavity's shape. However, the investigations performed by Sato et al. did not include the cavity as a flame-holder. The cavity was only used to produce the mixing enhancing acoustic waves.

Few, if any, experimental studies have investigated the acoustic properties of these cavities as they assist in mixing and the enhancement of combustion at lean conditions. This investigation is broken into three parts, which together will provide a clear interpretation of a cavity's suitability as an effective flame holder during weak combustion conditions. The first part of the investigation isolates the acoustic properties of the cavities. The frequency of a cavity can be estimated using an empirical equation derived by Heller and Delfs [6], as shown in Equation 1.1. This equation is estimated to be able to predict the frequency within the cavity $\pm 10\%$ [6].

$$f_m = \frac{m - \alpha}{\{M_\infty / \sqrt{1 + [(\gamma_\infty - 1)/2]M_\infty^2} + 1/k\}} \cdot \frac{U_\infty}{L} \quad (1.1)$$

1.1.1 Subsection 1

Nunc posuere quam at lectus tristique eu ultrices augue venenatis. Vestibulum ante ipsum primis in faucibus orci luctus et ultrices posuere cubilia Curae; Aliquam erat volutpat. Vivamus sodales tortor eget quam adipiscing in vulputate ante ullamcorper. Sed eros ante, lacinia et sollicitudin et, aliquam sit amet augue. In hac habitasse platea dictumst.

1.1.2 Subsection 2

Morbi rutrum odio eget arcu adipiscing sodales. Aenean et purus a est pulvinar pellen-
tesque. Cras in elit neque, quis varius elit. Phasellus fringilla, nibh eu tempus venenatis,
dolor elit posuere quam, quis adipiscing urna leo nec orci. Sed nec nulla auctor odio
aliquet consequat. Ut nec nulla in ante ullamcorper aliquam at sed dolor. Phasellus
fermentum magna in augue gravida cursus. Cras sed pretium lorem. Pellentesque eget
ornare odio. Proin accumsan, massa viverra cursus pharetra, ipsum nisi lobortis velit,
a malesuada dolor lorem eu neque.

1.2 Main Section 2

Sed ullamcorper quam eu nisl interdum at interdum enim egestas. Aliquam placerat
justo sed lectus lobortis ut porta nisl porttitor. Vestibulum mi dolor, lacinia molestie
gravida at, tempus vitae ligula. Donec eget quam sapien, in viverra eros. Donec pellen-
tesque justo a massa fringilla non vestibulum metus vestibulum. Vestibulum in orci quis
felis tempor lacinia. Vivamus ornare ultrices facilisis. Ut hendrerit volutpat vulputate.
Morbi condimentum venenatis augue, id porta ipsum vulputate in. Curabitur luctus
tempus justo. Vestibulum risus lectus, adipiscing nec condimentum quis, condimentum
nec nisl. Aliquam dictum sagittis velit sed iaculis. Morbi tristique augue sit amet nulla
pulvinar id facilisis ligula mollis. Nam elit libero, tincidunt ut aliquam at, molestie in
quam. Aenean rhoncus vehicula hendrerit.

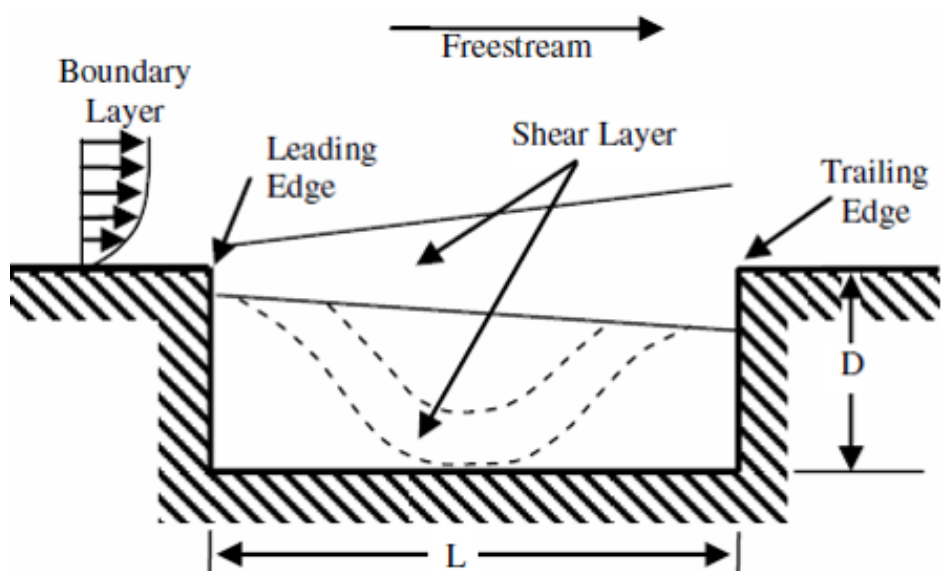


FIGURE 1.1: Typical hypersonic cavity schematic [11].

Chapter 2

Experimental Setup

2.1 Expansion Tube

The expansion tube is an impulse flow device similar to a shock tube. With an expansion tube, a high pressure gas is used to accelerate a volume of lower pressure gas to certain conditions required for supersonic testing. For the case of supersonic cavities, these conditions need to be similar to those found in the combustor of a scramjet engine.

WRITE THE CONDITIONS.

2.1.1 Sections

The expansion tube consists of four sections, which are highlighted in Figure 2.1. The four sections are: the driver, the double diaphragm, the driven, and the expansion, as listed from upstream to downstream. Initial conditions of the tube set by the operator determines test conditions within test section. These initial conditions include pressure ratios between the sections as well as the gases used in the sections.

The driver section is contained at a high pressure at the start of a test. This section is rated to be filled up to 800 psi. Non-combusting tests performed were run with a driver pressure of 225 psi. With higher pressures, faster test velocities of the test gas can be achieved.

2.1.2 Diaphragms

To separate the four sections, plastic diaphragms were placed at the boundary between these sections. These diaphragms were used to keep a pressure differential between the driver, double diaphragm, and driven sections. The pressure differential between these sections was a maximum of 120 psi for non-combusting tests. Another diaphragm was used to separate the test gas in the driver and the expansion gas in the expansion section. Depending on the test conditions, this diaphragm was required to withstand a maximum pressure differential of 1 psi.

Different thickness diaphragms were required, depending on the pressure differential between the sections. All diaphragms used for the driver and double diaphragm sections were cut from polycarbonate sheet. In order to determine the required diaphragm thickness, calculations were performed, utilizing known material properties and **SOME RELATIONSHIP**. Since the diaphragm is expected to expand to a near half sphere before breaking, a thin wall spherical pressure vessel relationship was used to determine the maximum pressure the plastic could withstand. This relationship, shown in Equation 2.1, was utilized to determine a range of thicknesses of the polycarbonate sheets to be used for different pressure conditions.

$$\sigma_{uts} = \frac{P r}{2t} \quad (2.1)$$

Thickness (inches)	Trial 1 Burst Pressure (psi)	Trial 2 Burst Pressure (psi)
0.010	32	n/a
0.015	60	n/a
0.020	93	92
0.030	123	125
0.045	153	163
1/16	233	274
3/32	341	n/a

TABLE 2.1: Diaphragm burst pressures at various thicknesses of polycarbonate sheets.

After initial testing of these diaphragms, it was determined this relationship provided an overestimation of about 185% for the breaking pressure of a specific thickness of diaphragm. Since the polycarbonate sheets come in certain stock thicknesses, several thicknesses were purchased and testing was performed to determine the breaking pressure of each diaphragm. For this testing, a 1/4" polycarbonate sheet was placed at the upstream end of the double diaphragm and the thinner test sample was placed at the downstream end of the double diaphragm. The double diaphragm was then filled slowly. When the downstream diaphragm broke, the highest pressure reached was recorded. This procedure was repeated for other thicknesses of diaphragms. The results from these burst tests is shown in Table 2.1. A majority of the non-combusting tests run were at a driver pressure of 225 psi, so 0.045" diaphragms were selected, as they have a higher burst pressure than the pressure differential between the driven and the double diaphragm, but not higher than the differential between the driver and the driven sections. These diaphragms reliably broke for each test.

Occasionally, after a test was run, it was noticed that the pieces of the diaphragm completely broke off, sending these pieces down the tube. Having these large pieces of diaphragm sent down the tube is unwanted. These large pieces can cause serious damage to the model in the test section, as well as damage to other parts of the tube. During one test, a large piece of diaphragm struck the nose of the blunted cylinder

model, causing severe damage to the pressure transducer located at the nose. It was also observed that pieces of diaphragm nicked the observation windows on the test section. These damages needed to be avoided, so one proposed solution to this problem was to score the diaphragms. A short, shallow incision on the outside of the plastic in an "X" pattern would create failure modes which the diaphragm should break along. These failure modes cause the diaphragm to petal, ideally opening as wide as the tube, with the entire diaphragm intact.

Burst tests were performed on several scored diaphragms of 0.045" thickness. This scoring was performed by hand with a knife, applying light pressure. The resulting score appeared as deep scratches in an "X" pattern. The results of the tests showed no significant decrease in burst pressure. In fact, all of the tests showed a higher burst pressure for the scored diaphragms than for the not scored ones. This could be due to the scoring allowing the plastic to deform further before bursting. It could also be due to the plastic being from a different batch sheet than the plastic used for earlier burst tests. Regardless of the reason, the results showed that the scored diaphragms could still be used. It was also found that good petalling of the diaphragm occurred, with minimal, if any, loss of diaphragm pieces down the tube. Because of these results, scoring of the diaphragms has become a regular step in the setup of the tube for each test.

2.1.3 •

2.2 Models

2.2.1 Overview and Design Choices

2.2.2 Modular Design

Because the acoustic properties are the main focus of this thesis, it was important to design a model in which these acoustic properties could change. Frequency is one main acoustic property that was chosen to be varied with these cavities. Using Heller and Delfs relationship, as stated previously, varying the length of the cavity would give different cavity frequencies [6]. However, the L/D is also an important parameter in the flame-holding characteristics of these cavities. Combining these need for various lengths with the need for certain range of L/D resulted in a modular design.

For the modular design, a 1/8-inch deep, 1 5/8-inch long cavity was created, as shown in Figure 2.2. The length of the cavity was chosen so that inserts could be attached, decreasing the overall length of the cavity, and achieving the desired L/D. Six inserts were manufactured to create L/Ds of 5, 7, and 9. These inserts are shown relative to the base cavity in Figure 2.3. At each L/D, there was one insert with a flat wall and one insert manufactured with a 30° incline. This angled incline, as shown by Ben-Yakar [2], has the ability to suppress the acoustic waves. This allowed for the comparison of flame-holding abilities of the cavity with and without strong acoustic waves present at each L/D. This modular design gave a relatively wide spectrum of cavity conditions to test with a relatively easy means of changing these conditions for each test.

2.2.3 Implementation

2.3 High Speed Pressure Transducers

Placed along the tube at various locations are piezoelectric pressure transducers. These pressure transducers provide both analog and digital data for each test run. The analog data allows for the observation of shock strength and the digital data allows for the calculation of shock velocity. The initial shock wave produced propagates down the tube. When the shock passes by one of these sensors, it registers as a very sharp increase in pressure. Knowing the time at which these shocks arrive at the various transducer locations, along with the location of the transducers relative to each other allows for the shock speed calculation.

In order to produce the digital signal required for the LabVIEW timer counter program to calculate the time between signals, a simple analog to digital circuit was designed. The design of the circuit was based off of previous work done by Helen Huches ???. This circuit, as shown in Figure ??, produces a 5V signal when an analog voltage is higher than a certain threshold. This threshold reference voltage is determined by three potentiometers connected to the circuit. The three potentiometers allow three different reference voltages to be set for up to six pressure transducer signals. When the analog voltage is lower than this reference voltage, the output of the circuit is 0V. This allows the digital data acquisition card to read either a HIGH (5V) signal or a LOW (0V) signal and interpret that as a digital signal.

This digital signal is also used to trigger the camera to record. The LabVIEW program, once getting a signal from a specified pressure transducer will generate a 5V TTL pulse. This pulse is

2.3.1 Circuit

2.3.2 Implementation and Troubleshooting

2.4 Infrared Sensor

Test time is one important metric needed for data analysis. After a test is run, the conditions of the test gas need to be known as well as for how long these conditions are experienced by the test gas. One way with which to determine that is with an infrared sensor.

The sensor used with the expansion tube at Lafayette is a Judson J10D series Indium Antemonide (InSb) sensor. These detectors have photovoltaic sensors that produce a current when exposed to infrared radiation.

2.4.1 Alignment

2.4.2 Calibration

2.4.3 Operation

To achieve the sensitivity required for the sensor, the operating temperature of the IR detector is about 77K. Because of this, the detector must be cooled with liquid nitrogen. Using the funnel to avoid spillage of the liquid nitrogen onto the cable connections or viewing window of the sensor, a few hundred milliliters were poured into the hole at the top of the sensor. When the sensor reaches the correct temperature, an eruption of cool gas occurs. It is important to wait until this eruption completes because the buildup of

gas can cause the cap to blow off. Once the eruption subsides, the cap can be replaced to the top of the sensor and power can be supplied to the amplifier.

2.5 Schlieren Imaging

The images captured for the tests were done so using a high speed camera with a schlieren system. A diagram of the schlieren system at Lafayette can be seen in Figure 2.6. The camera used for image capturing is a Phantom Miro m310 camera, capable of taking images up to 100 fps. However, as the recording frame rate increases, the resolution of each image decreases. For testing, a nominal frame rate of 77,000 kHz was used, as this provided a sufficient frame rate without sacrificing too much resolution.

The schlieren effect operates on the principle that light refracts in air due to changes in density. This can be observed firsthand on a hot day. The rippling effect one can see above a road on a hot day is the light refracting due to the different densities of the air, caused by differences in local air temperature. Schlieren imaging takes advantage of this principle by placing a knife edge at the focal point of the system. As light is refracted due to a change in density, this light gets blocked out by the knife edge, showing up as a dark spot in the captured image. Light that is not refracted continues through to the camera unblocked.

This type of imaging is important to see the various shock waves produced during testing. Since shock waves produce very sharp density gradients, a system that is capable of capturing these density gradients at high speeds is very useful. Typical test times experienced by the non-reacting tests were on the order of about 300 microseconds. With this camera, about 23 images were captured for the test time. With this many frames, it

was possible to time correlate the images as well as extract dominant frequencies within the cavities.

Further information about the system, including more detail on how the system works and how to calibrate and align the system at Lafayette can be found in Ray Sanzi's honors thesis [12].



FIGURE 2.1: Annotated photograph of the expansion tube at Lafayette College

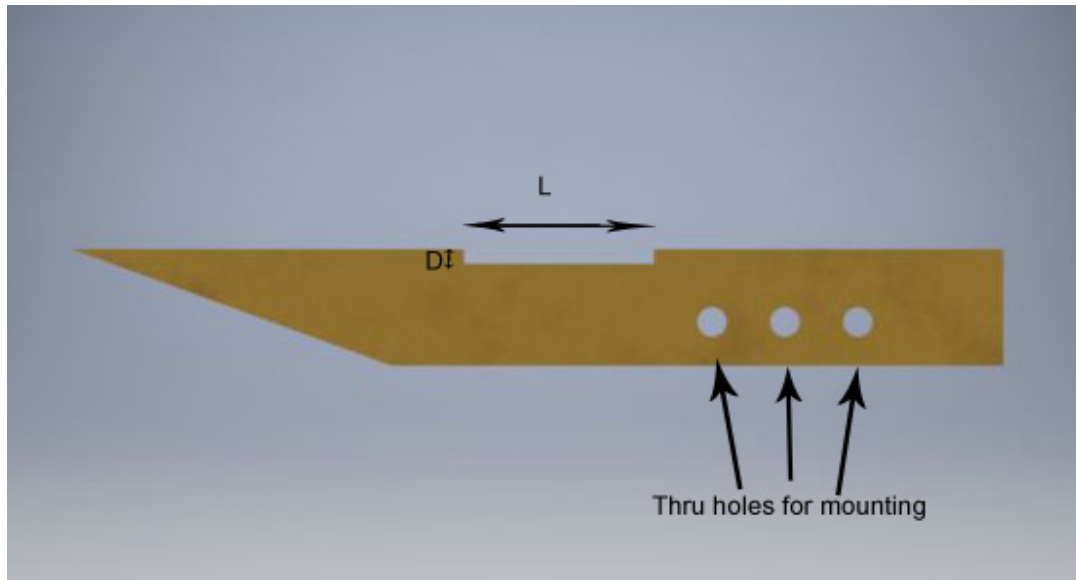


FIGURE 2.2: 3D rendering of cavity used in testing

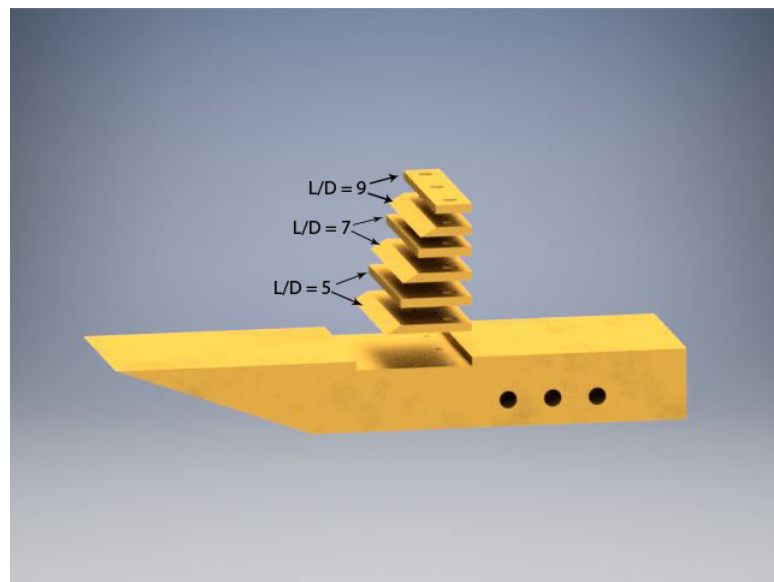


FIGURE 2.3: 3D rendering of cavity with various inserts to alter L/D

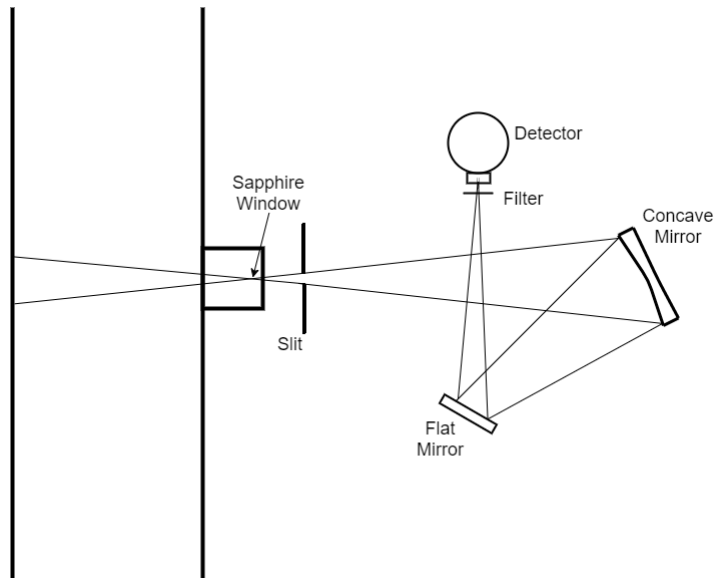


FIGURE 2.4: Schematic of the IR setup for the expansion tube.

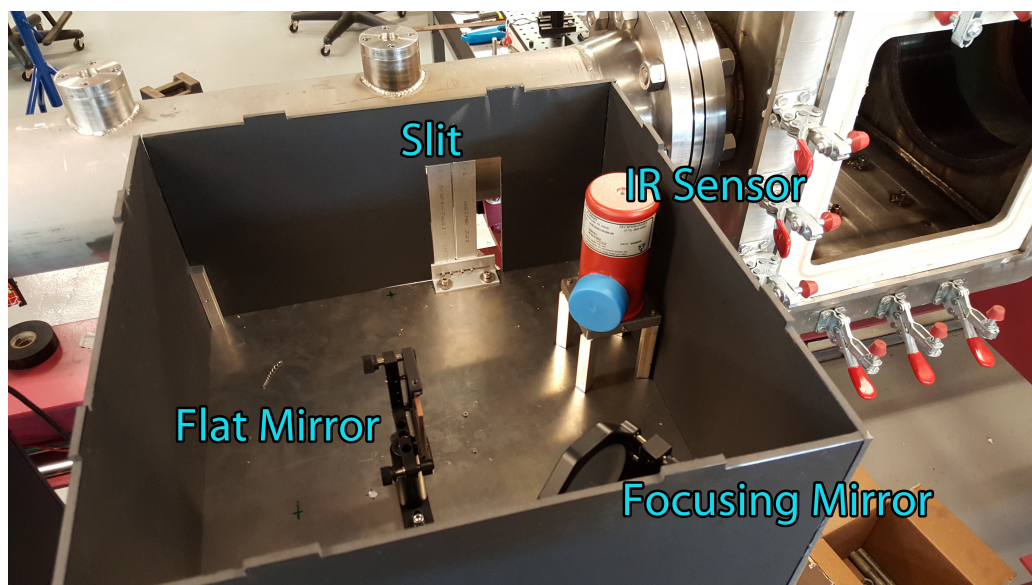


FIGURE 2.5: Photograph of actual IR setup in the lab.

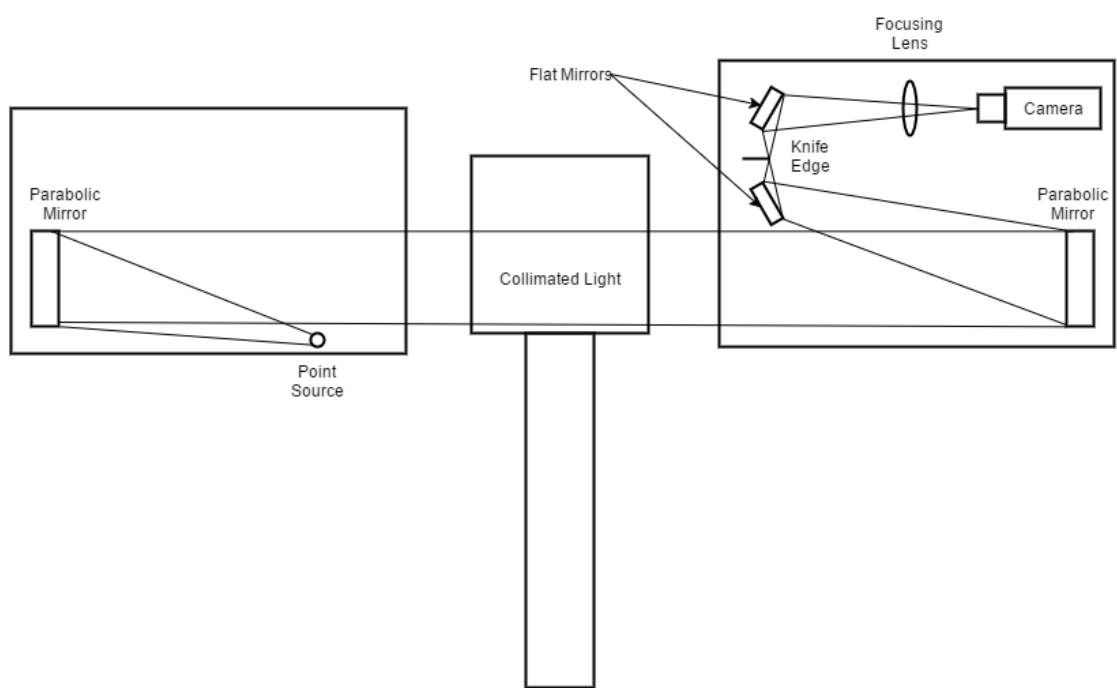


FIGURE 2.6: Diagram of schlieren system at Lafayette

Appendix A

Appendix Title Here

Write your Appendix content here.

Bibliography

- [1] Adela Ben-Yakar. *Experimental investigation of mixing and ignition of transverse jets in supersonic crossflows*. PhD thesis, Stanford University, 2000.
- [2] Adela Ben-Yakar and Ronald K Hanson. Cavity flame-holders for ignition and flame stabilization in scramjets: an overview. *Journal of Propulsion and Power*, 17(4):869–877, 2001.
- [3] Hyungrok Do. *Plasma-assisted combustion in a supersonic flow*. PhD thesis, Stanford University, 2009.
- [4] Ibrahim Yilmaz, Ece Ayli, and Selin Aradag. Investigation of the effects of length to depth ratio on open supersonic cavities using cfd and proper orthogonal decomposition. *The Scientific World Journal*, 2013, 2013.
- [5] O Haldun Unalmis. Cavity oscillation mechanisms in high-speed flows. *AIAA Journal*, 42(10):2035–2041, 2004.
- [6] H Heller and J Delfs. Letter to the editor: cavity pressure oscillations: the generating mechanism visualized. *Journal of Sound and Vibration*, 196(2):248–252, 1996.

- [7] David R Williams, Daniel Cornelius, and Clarence W Rowley. Supersonic cavity response to open-loop forcing. In *Active Flow Control*, pages 230–243. Springer, 2007.
- [8] O Wayne McGregor and RA White. Drag of rectangular cavities in supersonic and transonic flow including the effects of cavity resonance. *AIAA Journal*, 8(11):1959–1964, 1970.
- [9] ShiBin Luo, Wei Huang, Jun Liu, and ZhenGuo Wang. Drag force investigation of cavities with different geometric configurations in supersonic flow. *Science China Technological Sciences*, 54(5):1345–1350, 2011.
- [10] N Sato, A Imamura, S Shiba, S Takahashi, M Tsue, and M Kono. Advanced mixing control in supersonic airstream with a wall-mounted cavity. *Journal of Propulsion and Power*, 15(2):358–360, 1999.
- [11] Eli Lazar, Gregory Elliott, and Nick . Glumac. Control of the shear layer above a supersonic cavity using energy deposition. *AIAA journal*, 46(12):2987–2997, 2008.
- [12] Raymond Sanzi III. Working title. Honors thesis, 2016.